Aqueous photodegradation of substituted chlorobenzenes: Kinetics, carbon isotope fractionation, and reaction mechanisms

Elodie Passeport*[1,†‡], Ning Zhang[2, §], Langping Wu[2], Hartmut Herrmann[3], Barbara Sherwood Lollar[1], Hans-Hermann Richnow[2]

[1] Department of Earth Sciences, University of Toronto, 22 Russell Street, Toronto, ON M5S 3B1, Canada

Present addresses:

†Department of Civil Engineering, University of Toronto, 35 St George Street, Toronto, ON M5S 1A4, Canada

‡Department of Chemical Engineering and Applied Chemistry, University of Toronto, 200 College Street, Toronto, ON M5S 3E5, Canada

[2] Department of Isotope Biogeochemistry, Helmholtz Center for Environmental Research UFZ, Permoserstrasse 15, 04318 Leipzig, Germany

Present address:

§ Department of Chemistry and Pharmaceutical Engineering, Qilu University of Technology, Jinan 250353, China

[3] TROPOS Leibniz Institute for Tropospheric Research, Atmospheric Chemistry Department (ACD), Permoserstrasse 15, 04318 Leipzig, Germany

* Corresponding author

24 *Address: 35 St George Street, Room GB319F, M5S 1A4 Toronto ON Canada*

25 *Phone number: 001 416 978 5747*

26 *Fax number: 001 416 978 6813*

27 *Email address: elodie.passeport@utoronto.ca*

28

29

Abstract

Substituted chlorobenzenes are the basic substructure of many surface water contaminants. In this study, the isotope fractionation and reaction mechanisms involved during the aqueous direct and indirect photodegradation of CH_3-, Cl-, and NO_2- substituted chlorobenzenes were investigated in laboratory experiments. Only 4-nitrochlorobenzene showed slow but isotopically fractionating direct photolysis. During indirect photodegradation using UV/H_2O_2-generated OH radicals, the pseudo first-order reaction rate constants increased in the order of the NO_2- < Cl- < CH_3- substituted chlorobenzenes. The most pronounced carbon enrichment factors were observed for nitrochlorobenzenes (up to −4.8 ± 0.5‰), whereas the least significant were for chlorotoluenes (≤ −1.0 ± 0.1‰). As the substituents became more electron-withdrawing, the activation energy barrier increased, leading to slower reaction rates, and the transition state changed to a more symmetrical or less reactant-like structure, resulting in larger apparent kinetic isotope effects. The results suggest that the rate-determining step in the reaction with OH radicals was the addition of the electrophile to the benzene ring. Even though further research is needed to quantify isotope fractionation during other transformation processes, these results showed evidence that compound specific isotope analysis can be used as a diagnostic tool for the fate of substituted chlorobenzenes in water.

Keywords: photodegradation; water quality; chlorobenzenes; stable isotope; OH radicals

49 **TOC graphical abstract**

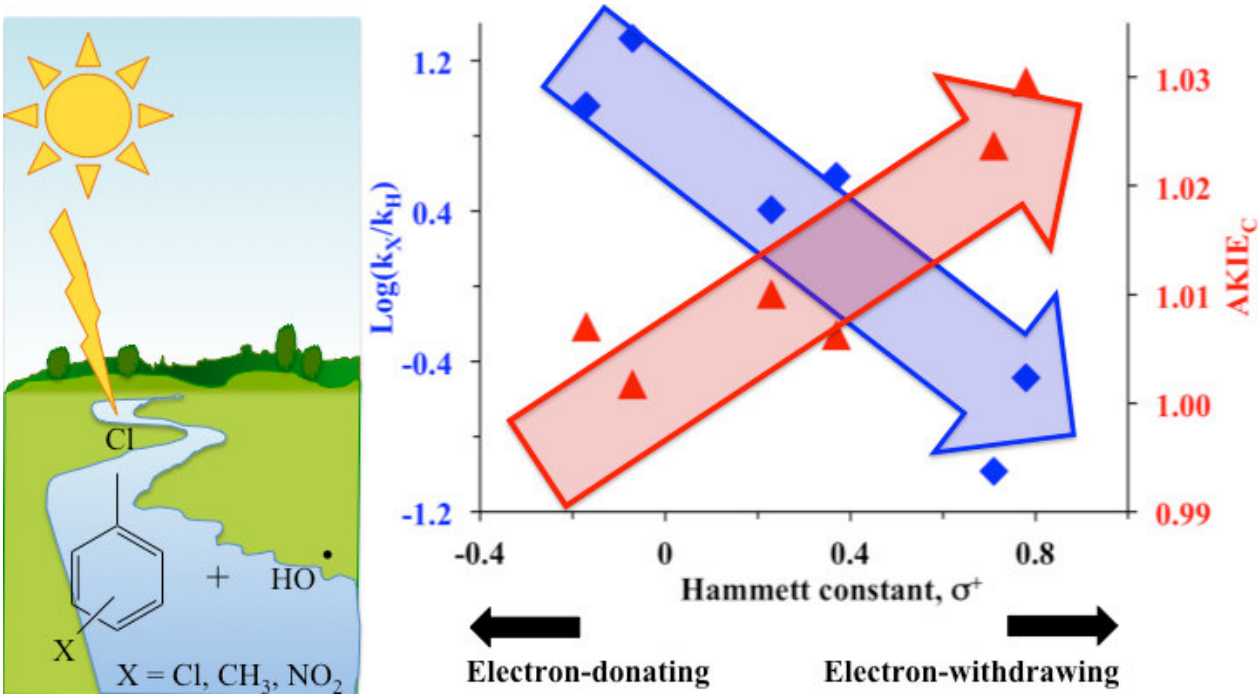

50
51

52 **Introduction**

53 Substituted chlorobenzenes are the basic chemical structure of many environmental contaminants
54 such as herbicides 2,4-D, dichlorprop, chlortoluron, and drugs and personal care products like
55 triclosan and diclofenac. In their simplest form, substituted chlorobenzenes, such as isomers of
56 dichlorobenzene (DCB), chloromethylbenzene (or chlorotoluene, CMB), and nitrochlorobenzene
57 (NCB), are widely distributed in surface waters (Schwarzbauer and Ricking 2010) in the low ng
58 L^{-1} or μg L^{-1} range (Bester et al. 1998, Lekkas et al. 2004, Trova et al. 1991), due to their use as
59 chemical intermediates in the production of dyes, solvents, pesticides, and pharmaceuticals. They
60 have all been listed as substances which could belong to List I of European Council Directive
61 76/464/EEC (European Commission 1982) due to their known or suspected toxicity to aquatic
62 organisms and mutagenic and carcinogenic potentials (Calamari et al. 1983, OECD 2005,
63 Shimizu et al. 1983, Weisburger et al. 1978). The dichlorobenzene isomers also belong to the
64 U.S. EPA List of Priority Pollutants (USEPA 1979). Characterizing the transfer and
65 transformation processes of substituted chlorobenzenes in surface waters is therefore essential to
66 protect human and aquatic life and develop effective remediation strategies. One method that can
67 be used to evaluate *in situ* transformation, Compound Specific Isotope Analysis (CSIA), is based
68 on the faster reaction rates of molecules containing light (e.g., ^{12}C) versus heavy (e.g., ^{13}C)
69 isotopes. While CSIA is widely used to study the fate and removal of traditional groundwater
70 contaminants, to date, its application to other environments such as sediments (Passeport et al.
71 2016) and surface waters is limited, e.g., Elsayed et al. (2014), Hartenbach et al. (2008), Maier et
72 al. (2016), and Ratti et al. (2015a). In some cases, CSIA can help identify transformation
73 processes that involve the breaking of chemical bonds. It can also be used to quantify

degradation and gain insight into contaminant reaction mechanisms without the need to identify transformation products (Hunkeler et al. 2008).

In natural environments such as lakes and rivers, and in water treatment plants where UV/H_2O_2 advanced oxidation processes are used, organic compounds can be eliminated via direct photolysis and indirect photolysis induced by reactive species such as hydroxyl (OH) radicals (Boreen et al. 2003, Wols and Hofman-Caris 2012). Hydoxyl radicals are naturally generated in all surface water environments from the photolysis of dissolved organic (Vaughan and Blough 1998) and inorganic compounds (Zafiriou 1974). Therefore, there is great potential to evaluate the attenuation of contaminants with OH radicals in various aquatic systems using CSIA, which could be a promising tool for water quality monitoring and assessment. One of the limitations of stable carbon isotope analysis is the need for about 0.2 – 20 ng of carbon to be injected on-column (Giebel et al. 2010), resulting in typically moderately high detection limits of 5 to 10 μg/L (Dempster et al. 1997, Hunkeler and Aravena 2000, Zwank et al. 2005), even though accurate carbon isotope analysis has been successfully conducted down to 0.1 – 1 μg/L (Schreglmann et al. 2013). The reaction mechanisms governing the direct and indirect photodegradation of substituted chlorobenzenes are not well understood. In addition, the potential of isotope fractionation during photodegradation reactions, and the extent to which it can contribute to deciphering reaction pathways have not been the subject of many studies. Previous research showed that stable carbon enrichment factors ranged from negligible values to ~ −5‰, e.g. during direct aqueous photolysis of polybrominated diphenyl ethers (Rosenfelder et al. 2011), organophosphorus pesticide dimethoate (Wu et al. 2014), herbicide atrazine (Hartenbach et al. 2008), and α-hexachlorocyclohexane (Zhang et al. 2014). Previous studies showed that direct photolytic dechlorination of the three chloroaniline isomers was associated

with highly variable carbon and nitrogen isotope effects, which depended on pH and excited spin state populations (Ratti et al. 2015b, Ratti et al. 2015c). Aqueous reactions of organic compounds with OH radicals also led to a similar range of stable carbon enrichment factors (Hartenbach et al. 2008, Ratti et al. 2015a, Wu et al. 2018, Zhang et al. 2014, Zhang et al. 2016, Zhang et al. 2015). For example, a negligible carbon enrichment factor (< ~ −0.5‰) was found during the reaction of OH radicals with atrazine (Hartenbach et al. 2008), as well as for toluene, ethylbenzene, xylenes, and anisole (Zhang et al. 2016); moderate values were obtained for α-hexachlorocyclohexane (−1.9‰) (Zhang et al. 2014) and fuel oxygenates (−1.0 to −1.6‰); while larger values, up to −3.9‰, were observed for anilines and nitrobenzene (Zhang et al. 2016). In some cases, the determination of isotope fractionation for two or more elements proved efficient to distinguish among degradation processes. The apparent kinetic isotope effect values for carbon and nitrogen for the direct (Ratti et al. 2015b, Ratti et al. 2015c) and indirect (Ratti et al. 2015a) photodegradation of chloroanilines correlated differently showing potential for the use of CSIA to differentiate between these chemical degradation pathways. However, the variability of isotope fractionation during aqueous photodegradation as a function of environmental conditions such as the type of reactive species, pH, and oxygen concentration (Hartenbach et al. 2008, Ratti et al. 2015a, Zhang et al. 2015), makes it difficult to predict reaction mechanisms and isotope effect for new molecules.

The objectives of this study were: 1) to estimate the extent of direct photolysis and indirect photolysis using OH radicals for substituted chlorobenzenes in aqueous solutions; 2) to quantify stable carbon isotope fractionation during photodegradation, 3) to evaluate the potential to use CSIA to differentiate aqueous photodegradation from other environmentally-relevant processes

119 such as biodegradation; and 4) to propose reaction mechanisms based on isotopic and kinetics
120 data.
121
122 **Materials and Methods**
123 ***Chemicals***
124 Hydrogen peroxide (H_2O_2, 30% w/w), n-pentane, and sodium chloride (NaCl) were obtained
125 from Merck (Darmstadt, Germany). The 1,2-, 1,3-, and 1,4-dichlorobenzene (1,2-, 1,3-, and 1,4-
126 DCB), 3- and 4-nitrochlorobenzene (3- and 4-NCB), and 3- and 4- chloro-methylbenzene (3- and
127 4-CMB) isomers were purchased from Sigma Aldrich. All chemicals were of analytical grade. A
128 solution of phosphate buffer (10 mM, pH = 7.3) was made with Na_2HPO_4 and NaH_2PO_4.
129 Ultrapure water (Milli-Q System, Millipore GmbH, Schwalbach/Ts. Germany) was used to
130 prepare the standards and pH buffer.
131
132 ***Photodegradation experiments***
133 All experiments were conducted using a 215-mL Pyrex cylindrical reactor vessel with a 28-cm^2
134 quartz window. The double-layer reactor wall allowed for controlling the reactor temperature at
135 20 °C. A 150-W xenon lamp (185 – 2,000 nm, L2175, Hamamatsu, Japan) was used with a filter
136 to cut-off radiations below 280 nm to better represent typical wavelengths at the Earth's surface.
137 The lamp was placed 10-cm away from the reactor. A schematic of the experimental system is
138 provided in Zhang et al. (2016). Each experiment was conducted with one of the studied
139 compounds with initial concentrations ranging from 2×10^{-4} to 7×10^{-4} M, similar to other
140 studies (Maier et al. 2016, Ratti et al. 2015a) and sufficiently low for the solutions to be
141 considered as optically dilute as per OECD Guideline 316 (OECD 2008) while guaranteeing

142 proper quantification of parent compounds and potential degradation products, and accurate
143 determination of stable carbon isotope signatures. Each solution was prepared in a pH = 7.3
144 aqueous phosphate buffer solution. For the indirect photodegradation experiments, 0.25 mL of
145 30% H_2O_2 was added to the solution at the start of the experiment, resulting in initial H_2O_2
146 concentrations of 12.5 mM, and contaminant to H_2O_2 molar ratios ranging between 1:50 and
147 1:25, similar to former studies (Daifullah and Mohamed 2004, Zhang et al. 2016) and
148 approximately one order of magnitude higher than for typical UV/H_2O_2 advanced oxidation
149 treatment processes (Collins and Bolton 2016). This ensured the formation of excess OH radials
150 therefore guaranteeing that direct photolysis and reactions with OH radical would dominate in
151 the reactors. A 200-mL volume of buffered solution was introduced in the reactor, leaving an
152 initial reactor headspace of 15 mL. The solution was continuously stirred at 500 rpm during the
153 experiment. Control dark experiments with 0.25 mL of 30% H_2O_2 were conducted for each
154 compound without light and covering the reactor with aluminum foil to prevent light penetration.
155 At each time step, 2 and 3 mL samples were collected for concentration and stable carbon
156 isotope analysis, respectively. At the end of each experiment, a 10-mL sample was collected for
157 product identification by gas chromatography mass spectrometry (GC/MS). The UV absorbance
158 peaks of all studied compounds were determined using a UV/VIS/NIR Lambda 900
159 spectrophotometer (Perkin Elmer Instruments) (Supplemental Information (SI) Figure S1 and
160 Table S1). Only a portion of 3-NCB and 4-NCB showed significant absorbance above 280 nm.
161
162 ***Analytical methods***

163 *Concentrations.* Concentrations of DCB, CMB, and NCB isomers were measured by gas
164 chromatography coupled to a flame ionization detector (GC/FID). Details on temperature
165 programs, sample preparation, and error estimation are provided in SI Section S2.
166
167 *Stable carbon isotope analysis*. For all compounds, the 3-mL samples collected for CSIA were
168 extracted with 0.5 mL of n-pentane by shaking on an orbital shaker for 1 hour at 200 rpm. The
169 extracts were immediately transferred to 2-mL vials with inserts and kept at −20 °C until
170 analysis. Stable carbon isotope values were determined by gas chromatography – combustion –
171 isotope ratio mass spectrometry (GC/C/IRMS, GC Isolink, ConFlo IV, and MAT 253), using a
172 ZB-1 column (60 m × 0.32 mm × 1 µm). The temperature program started at 40 °C, held for 5
173 min, then increased up to 280 °C at 20 °C min^{-1} and held for 2 min. A total error of ±0.5‰
174 encompassing accuracy and reproducibility was accounted for on each $\delta^{13}C$ value (Sherwood
175 Lollar et al. 2007).
176
177 *Product identification.* Photodegradation products were identified by gas chromatography (GC,
178 7890A, Agilent, Palo Alto, USA) mass spectrometry (MS, 5975C, Agilent, Palo Alto, USA). The
179 GC column was a HP-5 (30 m × 0.32 mm × 0.25 µm, Agilent), and the GC temperature program
180 started at 40 °C and held for 5 min, the temperature was then increased up to 90 °C at 3 °C min^{-1}
181 and held at 90 °C for 2 min, and increased up to 300 °C at 20 °C min^{-1} and held for 5 min.
182 Samples from the last sampling time of the direct and indirect photodegradation experiments
183 were analyzed after derivatization. Derivatization was conducted to identify potential phenolic
184 products as follows: 10 mg of $NaHCO_3$ was mixed into 1 mL of aqueous sample, and 5 µL of
185 acetic anhydride (0.05 M) was then added to acetylate phenolic groups. The mixture was shaken

186 for 20 min at 150 rpm and 0.5 mL of dichloromethane (DCM) was added before shaking again at
187 500 rpm for 1 hour. The DCM extracts were analyzed by GC/MS. Selected samples, collected
188 before the last sampling time for concentration measurement of the parent products, were also
189 analyzed by GC/MS without prior derivatization.
190
191 ***Hammett relationship***
192 A Hammett plot was constructed using the pseudo first-order rate constants with respect to the
193 aromatic compound (k_X) obtained from the indirect photodegradation experiments for each
194 chlorobenzene with substituent X placed in *meta* or *para* positions, i.e., X = Cl for 1,3-DCB and
195 1,4-DCB, CH_3 for the CMB isomers, and NO_2 for NCBs. The rate constants were normalized by
196 the chlorobenzene indirect photodegradation pseudo first-order rate constant, $k_H = 0.173\ h^{-1}$,
197 determined under the same experimental conditions by Zhang et al (2016). The Hammett
198 equation, $\log(k_X/k_H) = \rho\times\sigma$, was fitted to the data and parameter ρ, expressing the effect of a
199 substituent on the rate constant, was determined graphically. The Hammett substituent constants,
200 σ^+, for *meta* (σ^+_m) and *para* (σ^+_p) substituents, representing the total polar effect exerted by a
201 substituent on the reaction center when a positive charge is delocalized, were obtained from
202 Hansch et al. (1991). Due to steric hindrance, the Hammett relationship is not applicable to
203 *ortho*-substituted compounds such as 1,2-DCB.
204
205 ***Isotope data analysis***
206 Carbon enrichment factors (ε_C) were determined from the Rayleigh equation, Eq. (1), using the
207 linear regression of $\ln(R/R_0)$ as a function of $\ln(f)$, without forcing through zero, where R and R_0
208 are the isotopic compositions at any time $t > 0$ and the initial time t_0, and f is the fraction of

209 remaining compound at time t, calculated based on the stepwise correction method reported by
210 Buchner et al. (2017), even though virtually no difference were observed in the enrichment
211 factors when determined using the ratio of the concentrations at times t and t_0 for *f*:

212 $$\frac{R}{R_0} = (f)^{\varepsilon_C} \quad \text{Eq. (1)}$$

213 The enrichment factors represent carbon isotope effects for the whole molecule. To characterize
214 the isotope effect at the reactive position for each substituted chlorobenzene, apparent kinetic
215 isotope effect values for carbon ($AKIE_C$) were calculated as in Eq. (2) (Elsner et al. 2005):

216 $$\frac{1}{AKIE_C} = \frac{z \cdot n \cdot \varepsilon_C}{x \cdot 1000} + 1 \quad \text{Eq. (2)}$$

217 where, for a given postulated reaction mechanism, *n* is the number of carbon atoms in the
218 molecule, *x* is the number of carbon atoms at reactive positions, and *z* is the number of carbon
219 atoms at reactive positions with equal reactivity. Assuming negligible contribution from
220 secondary kinetic isotope effects (KIE_C), i.e., the reactive positions are associated with primary
221 isotope effect only, $x = z$.

222

223 **Results**

224 ***Control dark experiments***

225 The control dark experiments were conducted for each of the studied chemicals in presence of
226 H_2O_2. No significant concentration decrease was observed other than the expected headspace
227 losses of < 7% due to liquid – gas phase re-equilibration after each sampling (SI Figure S2). This
228 suggests that the sole presence of H_2O_2 does not induce degradation of the studied chemicals
229 under the experimental conditions used.

230

231 ***Direct photolysis***

232 In general, direct photolysis through UV light absorption (for $\lambda \geq 280$ nm) did not significantly
233 affect concentrations and isotope values (±0.5‰) of most studied compounds with two
234 exceptions (SI Figure S3). Direct photolysis of 1,4-DCB did not seem to produce significant
235 concentration decrease except during the 4 h and 19 h sampling times (Figure S3) during which
236 the light was off. Given that the subsequent samples showed constant concentrations, and that the
237 $\delta^{13}C$ values were within ±0.5‰ for times 0 h, 19 h, and 24 h, this concentration decrease is not
238 due to direct photolysis. For the direct photolysis of 4-NCB, the $\delta^{13}C$ values remained within ±
239 0.5‰ of the initial value of −32.9‰ for 2 days. However, subsequently, 4-NCB $\delta^{13}C$ values
240 became significantly enriched in ^{13}C by up to 2.2‰ after 4 days, when 34% of the initial
241 concentration had disappeared (SI Figures S3 (d) and S4). This is due to the potential of 4-NCB
242 to partially absorb light at wavelengths higher than the cut-off filter at 280 nm (see SI Figure S1),
243 with a maximum absorbance at 281 nm, and a corresponding molar absorption coefficient ε_{281nm}
244 of 3,242 M^{-1} cm^{-1} applying the Beer-Lambert law. The 4-NCB direct photolysis was associated
245 with a first-order degradation rate constant of 0.0043 ± 0.0003 h^{-1} (R^2 = 0.97) and an enrichment
246 factor of −5.1 ± 0.4 ‰ (R^2 = 0.96) over the reduction of 34% of the initial compound (SI Figure
247 S4 and Table S2).
248
249 ***Indirect photolysis***
250 Figure 1 presents the kinetics of indirect photodegradation of the studied compounds reacting
251 with OH radicals. The reactions followed pseudo first-order kinetics with respect to each
252 contaminant, with R^2 values greater than 0.94 and pseudo first-order rate constants (k_X) that
253 increased in the order of NCBs (0.018 and 0.056 h^{-1}), DCBs (0.44 – 0.66 h^{-1}), and CMBs (1.57
254 and 3.58 h^{-1}) (see SI Table S2). This is in agreement with previously reported pseudo first-order

255 rate constants of related compounds at similar initial concentrations reacting in UV/H_2O_2
256 systems, with similar molar ratio and H_2O_2 initial concentrations, such as substituted benzenes
257 (Ghaly et al. 2001, Sundstrom et al. 1989, Weir et al. 1987), e.g. with values ranging from 0.01
258 h^{-1} for nitrobenzene to 0.50 h^{-1} for N,N-dimethylaniline (Zhang et al. 2016). The CMBs
259 degraded at the fastest rates with concentrations reaching below detection limit levels after 2 h
260 for 3-CMB and 3.5 h for 4-CMB. The calculated indirect photodegradation half-live ($\ln(2)/k_X$)
261 were 1.0 to 1.6 h for DCBs, 0.2 h for 3-CMB and 0.4 h for 4-CMB, and 39 and 12 h for 3-NCB
262 and 4-NCB, respectively.
263 The Hammett plot is shown in Figure 2. The linear relationship between $\log(k_X/k_H)$ vs. σ^+
264 showed a good fit (R^2 = 0.85), and displayed a negative Hammett ρ value of −2.1, suggesting
265 that the reaction rate increases with electron-donating groups. This is in line with the observed
266 lower half-live of CMBs compared to DCBs and NCBs, and with previous similar studies of the
267 reaction of substituted benzenes with OH radicals (Mohan et al. 1991).
268 The Rayleigh equation was applied as described in Eq. (1) to determine stable carbon isotope
269 enrichment factors. The CMB isotope enrichment factors were insignificant (< −1.0 ± 0.1 ‰),
270 those for the DCB isomers were −1.75 ± 0.04 (1,2-DCB), −1.0 ± 0.1 ‰ (1,3-DCB), and −1.7 ±
271 0.2 ‰ (1,4-DCB), whereas those for the NCBs were the highest, −3.9 ± 0.3 ‰ (3-NCB) and
272 −4.8 ± 0.5 ‰ (4-NCB) (SI Table S2 and Figure 1). The ε_C values of NCBs were consistent with
273 the −3.9 ± 0.2 ‰ value obtained by Zhang et al. (2016) for nitrobenzene aqueous reaction with
274 OH radicals.
275
276 ***Transformation products***

277 For each experiment, selected samples were analyzed by GC/MS to identify remaining
278 degradation products (SI Table S3). The analysis did not reveal any phenolic products except for
279 the reaction of the two CMB isomers with OH radicals for which 2-chloro-6 (or 5)-methylphenol
280 were detected. These results are not consistent with the reported phenolic products obtained from
281 OH radical reactions with substituted benzenes. This is likely due to a combination of two
282 factors: first, the samples that underwent derivatization prior to analysis were those from the last
283 sampling points, when the proportions of remaining parent contaminant and intermediate
284 metabolites such as phenolic products were low; second, the samples collected at intermediate
285 sampling points were analyzed without prior derivatization, which would have limited the
286 potential to detect phenolic compounds.
287
288 **Discussion**

289 ***Substituted chlorobenzenes are subject to aqueous photodegradation***

290 The first finding of this research is that the complete disappearance of the compounds within 2 to
291 48 h – up to ~315 h for 3-NCB, the generation of some phenolic degradation products in the case
292 of the CMB isomers, and the observed stable carbon isotope fractionation all demonstrate that
293 substituted chlorobenzenes are able to react with photo-induced OH radicals in aqueous solution.
294 The absence of significant amounts of degradation intermediates was partly explained by the
295 absence of derivatization for intermediate samples, but could also show that the degradation
296 products further degrade as well. The pseudo first-order degradation rate constants of 2,4-
297 dichlorophenol, a potential product of the reaction of 1,3-DCB with OH radicals, were found to
298 be 3.1 h^{-1} in H_2O_2/UV processes and 3.0 and 10.4 h^{-1} during direct photolysis under similar
299 initial concentration and pH conditions as those used in this study (Pera-Titus et al. 2004). This is

300 5 to 16 times larger than that of 1,3-DCB at 0.66 ± 0.02 h^{-1} measured here, and therefore
301 suggests that detection of phenolic products would have been difficult due to their fast
302 degradation in the reactor.
303 The second finding of this study is that 4-NCB can also degrade directly via photolysis even in
304 the absence of reactive species such as OH radicals. However, this process was much slower (k =
305 0.0043 ± 0.0003 h^{-1}) than the reaction of 4-NCB with OH radicals (k = 0.056 ± 0.001 h^{-1}) and
306 therefore might not be relevant when both processes occur concurrently.
307
308 ***Insight into reaction mechanisms***
309 *Hammett plot*
310 The kinetics results showed a linear relationship between $\log(k_X/k_H)$ and σ^+ with a good
311 correlation coefficient (R^2 = 0.85) (Figure 2). This suggests that the reaction of substituted
312 chlorinated benzenes with OH radicals involves one main rate-determining step. The relatively
313 high magnitude of the proportionality constant, ρ, with an absolute value greater than 1, shows
314 that the effect of the substituents on the reaction rate is significant. The fact that the ρ value is
315 negative, −2.1, indicates that the reaction rates increase with electron-donating groups (CH_3) and
316 decrease with electron-withdrawing groups (Cl, NO_2). This is simply another way to note that the
317 reaction rates increase in the order of NO_2-, Cl-, and CH_3-substituted chlorobenzenes. Mohan et
318 al. (1991) studied OH radical addition to substituted chlorobenzenes, with $–CH_3$ and $–OCH_3$ as
319 electron-donating groups, and $–CF_3$, $–CHCl_2$, and $–CH_2Cl$ as electron-withdrawing groups.
320 Using a similar Hammett plot approach, they also obtained a negative but smaller slope of –0.52.
321 Other studies reported ρ values of –0.41 and –0.5 for the reaction of monosubstituted benzenes
322 with OH radicals (Anbar et al. 1966, Neta and Dorfman 1968). A negative value for ρ suggests

323 that a positive charge develops at the reaction center in the transition state of the rate-
324 determining step of the reaction of substituted chlorinated benzenes with OH radicals. This is a
325 characteristic of Electrophilic Aromatic Substitution (EAS) reactions. It is well established that
326 OH radical attack on aromatic compounds proceeds via a mechanism analogous to EAS (Anbar
327 et al. 1966). For such reactions, electron-withdrawing groups (e.g., Cl, NO_2) increase the energy
328 barrier for the addition of an electrophile, in this case the OH radical, to the aromatic ring. This is
329 due to a combination of transition state destabilization and ground state stabilization, and results
330 in a decrease in the reaction rate. Electrophilic aromatic substitution reactions are a two-step
331 process. For the reaction of substituted chlorobenzenes with OH radicals, the first step is rate
332 determining and involves the formation of a π complex transition state followed by the addition
333 of the OH radical and results in the formation of a sigma complex hydroxycyclohexadienyl
334 radical intermediate. The second step consists of the fast elimination of a H atom from the ring to
335 regain its aromaticity leaving a chlorophenolic product (Smith and Norman 1963).
336 The addition of OH radical to the ring and further elimination of a hydrogen atom to recover the
337 ring's aromaticity have been observed during the aqueous reaction of chlorotoluene (Mohan et
338 al. 1991) and nitrochlorobenzene with OH radicals that produced phenolic intermediate
339 compounds (Guittonneau et al. 1990). Zhang et al. (2016) also identified phenolic intermediates
340 in the reaction of substituted benzenes with OH radicals. In the present study, phenolic products
341 were observed in the early stage (< 2 h) of the reaction of 3- and 4-CMB with OH radicals, with
342 the production of 2-chloro-6-methylphenol and 2-chloro-5-methylphenol, respectively. This
343 confirms that OH addition to the ring is the most likely rate-determining step in the reaction of
344 the studied substituted chlorobenzenes with OH radicals.
345

346 *Isotope effects*

347 To further elucidate reaction mechanisms, $AKIE_C$ values were calculated to characterize the
348 isotope effect of the cleavage of the chemical bond at the reactive positions. Based on the
349 kinetics results discussed above, and former results on CMB and NCB (Guittonneau et al. 1990,
350 Mohan et al. 1991), OH radical aromatic substitution is expected to be the dominant mechanism
351 for the indirect photodegradation of the substituted chlorobenzenes. However, Zhang et al.
352 (2016) showed that the methyl group in toluene could also undergo H abstraction during reaction
353 with OH radicals, which could be expected for the CMB isomers. However, reaction products
354 following attack on the methyl group, such as 3- and 4-chlorobenzaldehyde and benzyl alcohols,
355 were not observed in the present study, while chlorophenols were observed for 3- and 4-CMBs.
356 To further evaluate if H abstraction was significant, in the $AKIE_C$ value calculations, two main
357 reaction pathways were hypothesized: OH radical substitution to a H atom attached to one of the
358 unsubstituted carbon atom of the benzene ring, and H abstraction from the methyl group in the
359 CMB isomers. In addition, instead of only considering all unsubstituted carbon atoms from the
360 benzene ring as potential reactive positions, the values for x and z in Eq. (2) for the calculation of
361 the $AKIE_C$ values were determined by considering the substituents' *ortho*-, *meta*-, or *para*-
362 directing effect, and whether they were activating or deactivating substituents on the benzene
363 ring (see details in SI Section S5). The calculated $AKIE_C$ values are summarized in SI Table S2.
364 By analogy with the conceptual framework developed for enzyme-catalyzed reactions, we can
365 represent the reaction of the X-substituted chlorobenzenes with OH radicals as shown in Scheme
366 1, where a hydroxycyclohexadienyl radical intermediate is formed:

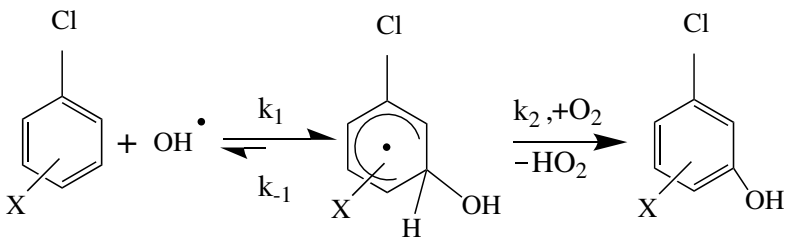

Scheme 1: OH radical ring substitution on X-substituted chlorobenzenes (X = CH_3, Cl, or NO_2)

This let us introduce a commitment factor, C, such that C = k_2/k_{-1} in the expression of $AKIE_C$:

$$AKIE_C = \frac{KIE_C + C}{1 + C} \qquad \text{Eq. (3)}$$

where KIE_C is the intrinsic kinetic isotope effect that depends only on the irreversible reaction step:

$$KIE_C = \frac{k_2^L}{k_2^H} \qquad \text{Eq. (4)}$$

Equation (3) assumes that the first reversible step is associated with negligible isotope effects. As it is not expected for k_{-1} to be significant, i.e., the addition of the OH radical to the aromatic ring is not easily reversible, $k_2 >> k_{-1}$, resulting in large values for C regardless of the substituent and its position. With large C values – equivalent to a very efficient enzymatic reaction – the $AKIE_C$ values are reduced (masked) and tend to be closer to unity rather than representing the intrinsic KIE_C.

All $AKIE_C$ values showed normal kinetic isotope effects ($AKIE_C > 1$) (SI Table S2). Under the assumption of OH radical electrophilic aromatic substitution, the $AKIE_C$ values were very close to unity for the DCB and CMB isomers, and somewhat higher for 3-NCB (1.024 ± 0.004) and 4-NCB (1.030 ± 0.004).

The absolute magnitude of the enrichment factors and the $AKIE_C$ values for the *meta*-substituted chlorobenzenes were always lower than those of their *para*-substituted counterparts. Given that

387 the *meta*-substituted chlorobenzenes reacted faster than their *para*-substituted counterparts, C_{meta}
388 > C_{para}, this resulted in the observed lower $AKIE_{Cmeta}$ than $AKIE_{Cpara}$ and therefore more
389 masking of the intrinsic KIE_C in the *meta*-substituted chlorobenzenes compared to their *para*-
390 substituted counterparts.
391 Theoretical and experimental KIE_C values obtained for C–O bond formation on alkenes typically
392 range from 0.998 to 1.024 for chemical oxidations with permanganate and epoxidation reactions
393 (Elsner et al. 2005, Singleton et al. 1997, Singleton and Wang 2005). The oxidation on a ring can
394 be expected to be associated with even larger KIE_C values due to the larger energy barrier of the
395 reaction to break a ring's aromaticity. Indeed, reported experimental $AKIE_C$ values for C–O
396 bond formation during ring hydroxylation ranged from 1.005 to 1.026 in biodegradation
397 experiments, and from 1.029 to 1.051 for abiotic experiments of gas-phase OH radical addition
398 to various aromatic compounds (SI Table S4). To the best of our knowledge, the only theoretical
399 KIE_C values calculated for the ring addition of OH radicals are those reported in Zhang et al.
400 (2016) for OH addition to the *para* position of various substituted benzenes, and ranged from
401 1.0239 to 1.0316. While the $AKIE_C$ values of the two NCB isomers were within these ranges,
402 those for the CMB and the DCB isomers were lower (1.002 – 1.011), possibly due to a masking
403 effect. Given that the reactor was continuously stirred, the reaction rates were expected to be
404 diffusion-controlled. Possible explanations proposed for the masking of the KIE_C in substituted
405 benzenes (Zhang et al. 2016) could apply here as well, such as the formation of the π complex
406 transition state prior to OH radical addition in Step 1 of Scheme 1, and pre-equilibrium between
407 the substituted chlorobenzene and the OH radical prior to the rate-determining step. A recent
408 study proposed that the creation of a water cage could account for masking of intrinsic KIE
409 (Kopinke and Georgi 2017). This cage effect was explained by the trapping of the OH radical

410 and substrate in the water shell formed by complex interaction of the hydrophobic solute with the
411 surrounding water molecules. The correlation between $AKIE_C$ values and molecules'
412 hydrophobicity ($\log(K_{ow})$ values) was used to evaluate this assumption. A good correlation (r^2 =
413 0.83) was found for the molecules studied in the present study (SI Figure S5). However a poor
414 correlation (r^2 = 0.46) was obtained when analyzing the dependency of $AKIE_C$ of substituted
415 benzenes using data from Zhang et al. (2016) (SI Figure S5) suggesting that the molecular
416 structure of the organic substrate was the main factor driving fractionation. The relationship
417 between $AKIE_C$ values and substituents' Hammett constants suggests that the electronic structure
418 of the organic molecules was the major factor governing isotope fractionation for radical
419 reactions in water. More research may be needed to validate the cage effect as a potential
420 contributor to KIE_C masking in OH radical aqueous reactions.
421 Under the scenario of OH radical addition to a substituted carbon atom, involving the breaking of
422 a C–Cl, C–N, or C–C bond, the same values for $AKIE_C$ as those for OH radical addition to an
423 unsubstituted carbon atom were obtained (SI Section S5). However, these $AKIE_C$ values were
424 significantly lower than the theoretical KIE_C Streitwieser limits for these cleavages, i.e. 1.057 for
425 C–Cl, 1.060 for C–N, and 1.049 for C–C (Elsner et al. 2005), which were obtained under the
426 assumption that the bond is broken during the transition state. When considering a more realistic
427 assumption, e.g. that the bond is 50% broken, half these limits can be considered. Even in this
428 case, the theoretical KIE_C values are still higher than the calculated $AKIE_C$ values, except for C–
429 N cleavage in the NCB isomers, confirming that the breaking of a C–X bond in the rate-
430 determining step is unlikely.
431 Finally, $AKIE_C$ values of 1.002 and 1.007 for 3- and 4-CMB, respectively, were obtained when
432 assuming hydrogen abstraction on the CH_3 group of the CMB isomers. These were lower than

433 theoretical KIE_C values of 1.020 expected for C–H bond cleavage (Elsner et al. 2005),
434 suggesting that OH radical addition to an unsubstituted carbon atom likely played a more
435 dominant role than hydrogen abstraction in the reaction of the CMB isomers with OH radicals.
436 This is in line with the higher contribution of OH addition relative to H abstraction observed for
437 toluene (Zhang et al. 2016). It is also confirmed by the detection of phenol intermediates in the
438 indirect photodegradation experiments with CMB isomers, which supports a preferential attack
439 of the OH radicals to the ring rather than the methyl group. Finally, this is also the main reaction
440 mechanism proposed for the reaction of chlorotoluene isomers with OH radicals in distilled
441 water (Mohan et al. 1991).
442 The ε_C and $AKIE_C$ values increased with increasing Hammett substituent constants σ^+ (Figure 3).
443 The most electron-withdrawing substituents led to the highest carbon isotope fractionation. This
444 suggests that the transition state might be more symmetrical for the reaction of OH radicals with
445 the NCB and DCB isomers than for the CMBs. More data are needed to propose a quantitative
446 relationship between isotope fractionation and substituent constants, and to provide a
447 mechanistic interpretation for such a relationship. The influence of the electronic properties of
448 aromatic substituents on isotope effects was observed for nitrogen isotope fractionation during
449 the oxidation of substituted anilines (Ratti et al. 2015a, Skarpeli-Liati et al. 2011, Skarpeli-Liati
450 et al. 2012) while no substituent effect was observed for the abiotic reduction of nitroaromatic
451 compounds (Hofstetter et al. 2008a).
452 Based on these kinetics and isotope results, the proposed dominant reaction pathway for the
453 studied compounds involves the initial formation of a C–O bond at one of the unsubstituted
454 carbon atoms on the benzene ring during the rate-determining step, followed by the release of a
455 hydrogen atom (Scheme 1).

456

457 ***Potential to use CSIA to distinguish between aqueous photodegradation and other processes***

458 The negligible isotope fractionation observed for the CMB isomers prevents stable carbon
459 isotope analysis to be used as an identification tool for CMB aqueous photodegradation.
460 Conversely, the NCBs, and to a lower extent the DCBs, showed quantifiable carbon isotope
461 fractionation during their reaction with OH radicals. While transformation reactions may produce
462 significant isotope fractionation, typically, negligible carbon isotope fractionation is associated
463 with transfer mechanisms such as equilibrium adsorption (Harrington et al. 1999, Passeport et al.
464 2014), diffusion (Passeport et al. 2014, Xu et al. 2016), and volatilization (Harrington et al.
465 1999), at least at scales relevant to most field sampling strategies (Xu et al. 2016, Xu et al. 2017).
466 Table S5 in SI summarizes published carbon isotope enrichment factors for various
467 transformation processes of substituted chlorobenzenes that could occur concurrently with
468 indirect photodegradation, e.g., microbial degradation under aerobic and anaerobic conditions,
469 abiotic processes, and direct photodegradation. Because significant gaps still exist in the
470 assessment of carbon isotope enrichment factors for these compounds, those of related
471 compounds were reported as well.

472 During anaerobic microbial degradation, 1,3-DCB and 1,4-DCB produce significant isotope
473 fractionation with ε_C values of −5.4 ± 0.4 and −6.3 ± 0.2 ‰, respectively, while 1,2-DCB is
474 associated with a low enrichment factor of −0.8 ± 0.1 ‰ (Liang et al. 2014). While the large ε_C
475 values of 1,3- and 1,4-DCB would prevent the use of stable carbon isotope analysis to
476 distinguish between anaerobic biodegradation and reaction with OH radicals, situations where
477 both processes occur simultaneously are rare. Indeed, indirect aqueous photodegradation is only
478 relevant in surface waters, where oxygenated conditions dominate. In aquatic surface

479 environments such as rivers, wetlands, and oceans, the concentrations in oxygen (Tao et al.
480 2006) and OH radicals (Zhou and Mopper 1990) decrease with depth, and anaerobic zones are
481 usually limited to the sediment phase or water depths at which reactions with OH radicals are not
482 expected. No carbon isotope enrichment factors have been reported for the aerobic
483 biodegradation of DCB isomers; however, negligible carbon isotope fractionation ($< -0.4 \pm 0.1$
484 ‰) was observed for chlorobenzene (Kaschl et al. 2005) and 1,2,4-trichlorobenzene (Griebler et
485 al. 2004, Liang et al. 2011), suggesting that DCBs might also be associated with small ε_C values
486 during aerobic biodegradation. There is therefore potential to use CSIA to identify indirect
487 aqueous photodegradation of the DCB isomers.
488 For NCBs, the only other published ε_C value, −0.65 ‰, is that associated with the abiotic
489 reduction of 4-NCB in suspensions of Fe(II)/goethite (Hartenbach et al. 2006). No information
490 on stable carbon isotope fractionation exists for the aerobic or anaerobic biodegradation of NCB
491 isomers. However, nitrobenzene was studied under aerobic conditions, and exhibited ε_C values of
492 -0.57 ± 0.06 ‰ during aerobic partial reduction by *Pseudomonas pseudoalcaligenes* strain JS45
493 (Hofstetter et al. 2008b), and between -3.5 ± 0.2 and -3.9 ± 0.2 ‰ for nitrobenzene aerobic
494 oxidation with various bacteria strains, cell extracts, and enzymes (Hofstetter et al. 2008b, Pati et
495 al. 2014). Smaller ε_C values were obtained for the aerobic oxidation of 2-, 3-, 4-, and 2,6-di-
496 nitrotoluene, ranging from -0.4 ± 0.2 and -1.4 ± 0.4 ‰ (Pati et al. 2014, Pati et al. 2016).
497 Altogether, these results suggest that the aerobic biodegradation of NCB isomers could produce
498 stable carbon isotope fractionation within a similar range as that reported here for their reaction
499 with OH radicals. These effects should be evaluated in future studies before CSIA can be used as
500 a diagnostic tool for NCB fate in surface water environments.
501

Conclusions

- Results from (i) the Hammett relationship, (ii) the stable carbon isotope analysis, (iii) degradation product analysis, and (iv) former literature studies provided multiple lines of evidence that the reaction of OH radicals with substituted chlorobenzenes proceeds primarily via OH aromatic substitution, involving first the rate-determining C–O bond formation, followed by H release.
- The substituents on the chlorobenzene structure affected both reactivity and stable carbon isotope fractionation.
- While the carbon isotope enrichment factors obtained in this study were small, they will likely be sufficient to identify indirect photodegradation of the NCB and potentially the DCB isomers provided that at least 40% of the NCBs and 70 – 87% of the DCBs degrade via reaction with OH radicals.
- In order to conclusively assess the diagnostic capabilities of CSIA for substituted chlorobenzenes, further research should be conducted with more complex water matrices.

Acknowledgements

This research has been financially supported by the European Union under the 7th Framework Program (project acronym CSI:ENVIRONMENT, contract number PITN-GA-2010-264329), and a Collaborative Research and Development grant from the Natural Sciences and Engineering Research Council of Canada (#497236).

Appendix A. Supplementary data

Supplementary data related to this article can be found at xxx.

References

Anbar, M., Meyerstein, D. and Neta, P. (1966) The reactivity of aromatic compounds toward hydroxyl radicals. The Journal of Physical Chemistry 70(8), 2660-2662.

Bester, K., Gatermann, R., Huhnerfuss, H., Lange, W. and Theobald, N. (1998) Results of non target screening of lipophilic organic pollutants in the German Bight. IV: Identification and quantification of chloronitrobenzenes and dichloronitrobenzenes. Environmental Pollution 102(2-3), 163-169.

Boreen, A.L., Arnold, W.A. and McNeill, K. (2003) Photodegradation of pharmaceuticals in the aquatic environment: A review. Aquatic Sciences 65(4), 320-341.

Buchner, D., Jin, B., Ebert, K., Rolle, M., Elsner, M. and Haderlein, S.B. (2017) Experimental determination of isotope enrichment factors - Bias from mass removal by repetitive sampling. Environmental Science & Technology 51(3), 1527-1536.

Calamari, D., Galassi, S., Setti, F. and Vighi, M. (1983) Toxicity of selected chlorobenzenes to aquatic organisms. Chemosphere 12(2), 253-262.

Collins, J. and Bolton, J.R. (2016) Advanced oxidation handbook, American Water Works Association, Denver, CO, USA.

Daifullah, A.H.A. and Mohamed, M.M. (2004) Degradation of benzene, toluene ethylbenzene and p-xylene (BTEX) in aqueous solutions using UV/H2O2 system. Journal of Chemical Technology and Biotechnology 79(5), 468-474.

Dempster, H.S., Sherwood Lollar, B. and Feenstra, S. (1997) Tracing organic contaminants in groundwater: A new methodology using compound-specific isotopic analysis. Environmental Science & Technology 31(11), 3193–3197.

Elsayed, O.F., Maillard, E., Vuilleumier, S., Nijenhuis, I., Richnow, H.H. and Imfeld, G. (2014) Using compound-specific isotope analysis to assess the degradation of chloroacetanilide herbicides in lab-scale wetlands. Chemosphere 99, 89-95.

Elsner, M., Zwank, L., Hunkeler, D. and Schwarzenbach, R.P. (2005) A new concept linking observable stable isotope fractionation to transformation pathways of organic pollutants. Environmental Science & Technology 39(18), 6896-6916.

European Commission (1982) Official Journal of the European Communities C176, Communication from the Commission to the Council on dangerous substances which might be included in List I of Council Directive 76/464/EEC, 14 July 1982, Volume 25, p. 14.

Ghaly, M.Y., Hartel, G., Mayer, R. and Haseneder, R. (2001) Photochemical oxidation of p-chlorophenol by UV/H2O2 and photo-Fenton process. A comparative study. Waste Management 21(1), 41-47.

Giebel, B.M., Swart, P.K. and Riemer, D.D. (2010) Delta 13-C table isotope analysis of atmospheric oxygenated volatile organic compounds by gas chromatography-isotope ratio mass spectrometry. Analytical Chemistry 82(16), 6797–6806.

Griebler, C., Safinowski, M., Vieth, A., Richnow, H.H. and Meckenstock, R.U. (2004) Combined application of stable carbon isotope analysis and specific metabolites determination for assessing in situ degradation of aromatic hydrocarbons in a tar oil-contaminated aquifer. Environmental Science & Technology 38(2), 617–631.

Guittonneau, S., De Laat, J., Guguet J.-P., Bonnel, C. and Dore, M. (1990) Oxidation of parachloronitrobenzene in dilute aqueous solution by O3 UV and H2O2 UV: A Comparative Study. Ozone: Science & Engineering 12(1), 73-94.

Hansch, C., Leo, A. and Taft, R.W. (1991) A survey of Hammett substituent constants and resonance and field parameters. Chemical Reviews 91(2), 165-195.

Harrington, R.R., Poulson, S.R., Drever, J.I., Colberg, P.J.S. and Kelly, E.F. (1999) Carbon isotope systematics of monoaromatic hydrocarbons: vaporization and adsorption experiments. Organic Geochemistry 30(8A), 765–775.

Hartenbach, A., Hofstetter, T.B., Berg, M., Bolotin, J. and Schwarzenbach, R.P. (2006) Using nitrogen isotope fractionation to assess abiotic reduction of nitroaromatic compounds. Environmental Science & Technology 40(24), 7710-7716.

Hartenbach, A.E., Hofstetter, T.B., Tentscher, P.R., Canonica, S., Berg, M. and Schwarzenbach, R.P. (2008) Carbon, hydrogen, and nitrogen isotope fractionation during light-induced transformations of atrazine. Environmental Science & Technology 42(21), 7751-7756.

Hofstetter, T.B., Neumann, A., Arnold, W.A., Hartenbach, A.E., Bolotin, J., Cramer, C.J. and Schwarzenbach, R.P. (2008a) Substituent effects on nitrogen isotope fractionation during abiotic reduction of nitroaromatic compounds. Environmental Science & Technology 42(6), 1997-2003.

Hofstetter, T.B., Spain, J.C., Nishino, S.F., Bolotin, J. and Schwarzenbach, R.P. (2008b) Identifying competing aerobic nitrobenzene biodegradation pathways by compound-specific isotope analysis. Environmental Science & Technology 42(13), 4764-4770.

Hunkeler, D. and Aravena, R. (2000) Determination of compound-specific carbon isotope ratios of chlorinated methanes, ethanes, and ethenes in aqueous samples. Environmental Science & Technology 34(13).

Hunkeler, D., Meckenstock, R.U., Sherwood Lollar, B., Schmidt, T.C. and Wilson, J.T. (2008) A guide for assessing biodegradation and source identification of organic ground water contaminants using Compound Specific Isotope Analysis (CSIA), p. 67, United States Environmental Protection Agency, Ada, OK.

Kaschl, A., Vogt, C., Uhlig, S., Nijenhuis, I., Weiss, H., Kastner, M. and Richnow, H.H. (2005) Isotopic fractionation indicates anaerobic monochlorobenzene biodegradation. Environmental Toxicology and Chemistry 24(6), 1315-1324.

Kopinke, F.D. and Georgi, A. (2017) What controls selectivity of hydroxyl radicals in aqueous solution? Indications for a cage effect. Journal of Physical Chemistry A 121(41), 7947-7955.

Lekkas, T., Kolokythas, G., Nikolaou, A., Kostopoulou, M., Kotrikla, A., Gatidou, G., Thomaidis, N.S., Golfinopoulos, S., Makri, C., Babos, D., Vagi, M., Stasinakis, A., Petsas, A. and Lekkas, D.F. (2004) Evaluation of the pollution of the surface waters of Greece from the priority compounds of List II, 76/464/EEC Directive, and other toxic compounds. Environment International 30(8), 995-1007.

Liang, X., Howlett, M.R., Nelson, J.L., Grant, G., Dworatzek, S., Lacrampe-Couloume, G., Zinder, S.H., Edwards, E.A. and Sherwood Lollar, B. (2011) Pathway-dependent isotope fractionation during aerobic and anaerobic degradation of monochlorobenzene and 1,2,4-trichlorobenzene. Environmental Science & Technology 45(19), 8321–8327.

Liang, X., Mundle, S.O.C., Nelson, J.L., Passeport, E., Chan, C.C.H., Lacrampe-Couloume, G., Zinder, S.H. and Sherwood Lollar, B. (2014) Distinct carbon isotope fractionation during anaerobic degradation of dichlorobenzene isomers. Environmental Science & Technology 48(9), 4844-4851.

Maier, M.P., Prasse, C., Pati, S.G., Nitsche, S., Li, Z., Radke, M., Meyer, A., Hofstetter, T.B., Ternes, T.A. and Elsner, M. (2016) Exploring trends of C and N isotope fractionation to trace transformation reactions of diclofenac in natural and engineered systems. Environmental Science & Technology 50(20), 10933-10942.

Mohan, H., Mudaliar, M., Aravindakumar, C.T., Rao, B.S.M. and Mittal, J.P. (1991) Studies on structure reactivity in the reaction of OH radicals with substituted halobenzenes in aqueous solutions. Journal of the Chemical Society-Perkin Transactions 2 (9), 1387-1392.

Neta, P. and Dorfman, L.M. (1968) Pulse Radiolysis Studies. XIII. Rate constants for the reaction of hydroxyl radicals with aromatic compounds in aqueous solutions. Advances in Chemistry 81, 222-230.

OECD (2005) p-chlorotoluene CAS N°: 106-43-4 Screening Information DataSheet - Initial assessment report for SIAM 20, p. 154, UNEP Publication.

OECD (2008) Organisation for Economic Co-operation and Development (OECD). Test guideline 316, Phototransformation of chemicals in water - Direct photolysis, p. 53.

Passeport, E., Landis, R., Lacrampe-Couloume, G., Lutz, E.J., Mack, E.E., West, K., Morgan, S. and Lollar, B.S. (2016) Sediment monitored natural recovery evidenced by compound specific isotope analysis and high-resolution pore water sampling. Environmental Science & Technology 50(22), 12197-12204.

Passeport, E., Landis, R., Mundle, S.O., Chu, K., Mack, E.E., Lutz, E. and Sherwood Lollar, B. (2014) Diffusion sampler for compound specific carbon isotope analysis of dissolved hydrocarbon contaminants. Environmental Science & Technology 48(16), 9582–9590.

Pati, S.G., Kohler, H.P.E., Bolotin, J., Parales, R.E. and Hofstetter, T.B. (2014) Isotope effects of enzymatic dioxygenation of nitrobenzene and 2-nitrotoluene by nitrobenzene dioxygenase. Environmental Science & Technology 48(18), 10750-10759.

Pati, S.G., Kohler, H.P.E., Pabis, A., Paneth, P., Parales, R.E. and Hofstetter, T.B. (2016) Substrate and enzyme specificity of the kinetic isotope effects associated with the dioxygenation of nitroaromatic contaminants. Environmental Science & Technology 50(13), 6708-6716.

Pera-Titus, M., Garcia-Molina, V., Banos, M.A., Gimenez, J. and Esplugas, S. (2004) Degradation of chlorophenols by means of advanced oxidation processes: a general review. Applied Catalysis B-Environmental 47(4), 219-256.

Ratti, M., Canonica, S., McNeill, K., Bolotin, J. and Hofstetter, T.B. (2015a) Isotope fractionation associated with the indirect photolysis of substituted anilines in aqueous solution. Environmental Science & Technology 49(21), 12766-12773.

Ratti, M., Canonica, S., McNeill, K., Bolotin, J. and Hofstetter, T.B. (2015b) Isotope fractionation associated with the photochemical dechlorination of chloroanilines. Environmental Science & Technology 49(16), 9797-9806.

Ratti, M., Canonica, S., McNeill, K., Erickson, P.R., Bolotin, J. and Hofstetter, T.B. (2015c) Isotope fractionation associated with the direct photolysis of 4-chloroaniline. Environmental Science & Technology 49(7), 4263-4273.

Rosenfelder, N., Bendig, P. and Vetter, W. (2011) Stable carbon isotope analysis (delta C-13 values) of polybrominated diphenyl ethers and their UV-transformation products. Environmental Pollution 159(10), 2706-2712.

Schreglmann, K., Hoeche, M., Steinbeiss, S., Reinnicke, S. and Elsner, M. (2013) Carbon and nitrogen isotope analysis of atrazine and desethylatrazine at sub-microgram per liter concentrations in groundwater. Analytical and Bioanalytical Chemistry 405(9), 2857-2867.

Schwarzbauer, J. and Ricking, M. (2010) Non-target screening analysis of river water as compound-related base for monitoring measures. Environmental Science and Pollution Research 17(4), 934-947.

Sherwood Lollar, B., Hirschorn, S.K., Chartrand, M.M.G. and Lacrampe-Couloume, G. (2007) An approach for assessing total instrumental uncertainty in compound-specific carbon isotope

661 analysis: Implications for environmental remediation studies. Analytical Chemistry 79(9), 3469-
662 3475.
663 Shimizu, M., Yasui, Y. and Matsumoto, N. (1983) Structural specificity of aromatic compounds
664 with special reference to mutagenic activity in Salmonella typhimurium: a series of chloro- or
665 fluoro-nitrobenzene derivatives. Mutation Research 116(3-4), 217-238.
666 Singleton, D.A., Merrigan, S.R., Liu, J. and Houk, K.N. (1997) Experimental geometry of the
667 epoxidation transition state. Journal of the American Chemical Society 119(14), 3385-3386.
668 Singleton, D.A. and Wang, Z.H. (2005) Isotope effects and the nature of enantioselectivity in the
669 shi epoxidation. The importance of asynchronicity. Journal of the American Chemical Society
670 127(18), 6679-6685.
671 Skarpeli-Liati, M., Jiskra, M., Turgeon, A., Garr, A.N., Arnold, W.A., Cramer, C.J.,
672 Schwarzenbach, R.P. and Hofstetter, T.B. (2011) Using nitrogen isotope fractionation to assess
673 the oxidation of substituted anilines by manganese oxide. Environmental Science & Technology
674 45(13), 5596-5604.
675 Skarpeli-Liati, M., Pati, S., Bolotin, J. and Hofstetter, T.B. (2012) Carbon, hydrogen, and
676 nitrogen isotope fractionation associated with oxidative transformation of substituted aromatic
677 N-alkyl amines. Environmental Science & Technology 46(13), 7189-7198.
678 Smith, J.R.L. and Norman, R.O.C. (1963) Hydroxylation. Part I. The oxidation of benzene and
679 toluene by Fenton's reagent. Journal of the Chemical Society, 2897-2905.
680 Sundstrom, D.W., Weir, B.A. and Klei, H.E. (1989) Destruction of aromatic pollutants by UV
681 light catalyzed oxidation with hydrogen peroxide. Environmental Progress 8(1), 6-11.
682 Tao, W.D., Hall, K.J. and Duff, S.J.B. (2006) Performance evaluation and effects of hydraulic
683 retention time and mass loading rate on treatment of woodwaste leachate in surface-flow
684 constructed wetlands. Ecological Engineering 26(3), 252-265.
685 Trova, C., Cossa, G. and Gandolfo, G. (1991) Behavior and fate of chloronitrobenzene in a
686 fluvial environment. Bulletin of Environmental Contamination and Toxicology 47(4), 580-585.
687 USEPA (1979) United States Environmental Protection Agency, List of priority pollutants, 40
688 Code of Federal Regulations Part 423, Appendix A., p. 1.
689 Vaughan, P.P. and Blough, N.V. (1998) Photochemical formation of hydroxyl radical by
690 constituents of natural waters. Environmental Science & Technology 32(19), 2947-2953.
691 Weir, B.A., Sundstrom, D.W. and Klei, H.E. (1987) Destruction of benzene by ultraviolet light-
692 catalyzed oxidation with hydrogen peroxide. Hazardous Waste & Hazardous Materials 4(2), 165-
693 176.
694 Weisburger, E.K., Russfield, A.B., Homburger, F., Weisburger, J.H., Boger, E., Vandongen,
695 C.G. and Chu, K.C. (1978) Testing of twenty-one environmental aromatic amines or derivatives
696 for long-term toxicity or carcinogenicity. Journal of Environmental Pathology and Toxicology
697 2(2), 325-356.
698 Wols, B.A. and Hofman-Caris, C.H.M. (2012) Review of photochemical reaction constants of
699 organic micropollutants required for UV advanced oxidation processes in water. Water Research
700 46(9), 2815-2827.
701 Wu, L.P., Chladkova, B., Lechtenfeld, O.J., Lian, S.J., Schindelka, J., Herrmann, H. and
702 Richnow, H.H. (2018) Characterizing chemical transformation of organophosphorus compounds
703 by C-13 and H-2 stable isotope analysis. Science of the Total Environment 615, 20-28.
704 Wu, L.P., Yao, J., Trebse, P., Zhang, N. and Richnow, H.H. (2014) Compound specific isotope
705 analysis of organophosphorus pesticides. Chemosphere 111, 458-463.

Xu, B.S., Sherwood Lollar, B., Passeport, E. and Sleep, B.E. (2016) Diffusion related isotopic fractionation effects with one-dimensional advective-dispersive transport. Science of the Total Environment 550, 200-208.

Xu, S., Sherwood Lollar, B. and Sleep, B.E. (2017) Rethinking aqueous phase diffusion related isotope fractionation: Contrasting theoretical effects with observations at the field scale. Science of the Total Environment 607-608, 1085-1095.

Zafiriou, O.C. (1974) Sources and reactions of OH and daughter radicals in seawater. Journal of Geophysical Research 79(30), 4491-4497.

Zhang, N., Bashir, S., Qin, J., Schindelka, J., Fischer, A., Nijenhuis, I., Herrmann, H., Wick, L.Y. and Richnow, H.H. (2014) Compound specific stable isotope analysis (CSIA) to characterize transformation mechanisms of alpha-hexachlorocyclohexane. Journal of Hazardous Materials 280, 750-757.

Zhang, N., Geronimo, I., Paneth, P., Schindelka, J., Schaefer, T., Herrmann, H., Vogt, C. and Richnow, H.H. (2016) Analyzing sites of OH radical attack (ring vs. side chain) in oxidation of substituted benzenes via dual stable isotope analysis (delta C-13 and delta H-2). Science of the Total Environment 542, 484-494.

Zhang, N., Schindelka, J., Herrmann, H., George, C., Rosell, M., Herrero-Martin, S., Klan, P. and Richnow, H.H. (2015) Investigation of humic substance photosensitized reactions via carbon and hydrogen isotope fractionation. Environmental Science & Technology 49(1), 233-242.

Zhou, X.L. and Mopper, K. (1990) Determination of photochemically produced hydroxyl radicals in seawater and fresh water. Marine Chemistry 30(1-3), 71-88.

Zwank, L., Berg, M., Elsner, M., Schmidt, T.C., Schwarzenbach, R.P. and Haderlein, S.B. (2005) New evaluation scheme for two-dimensional isotope analysis to decipher biodegradation processes: Application to groundwater contamination by MTBE. Environmental Science & Technology 39(4).

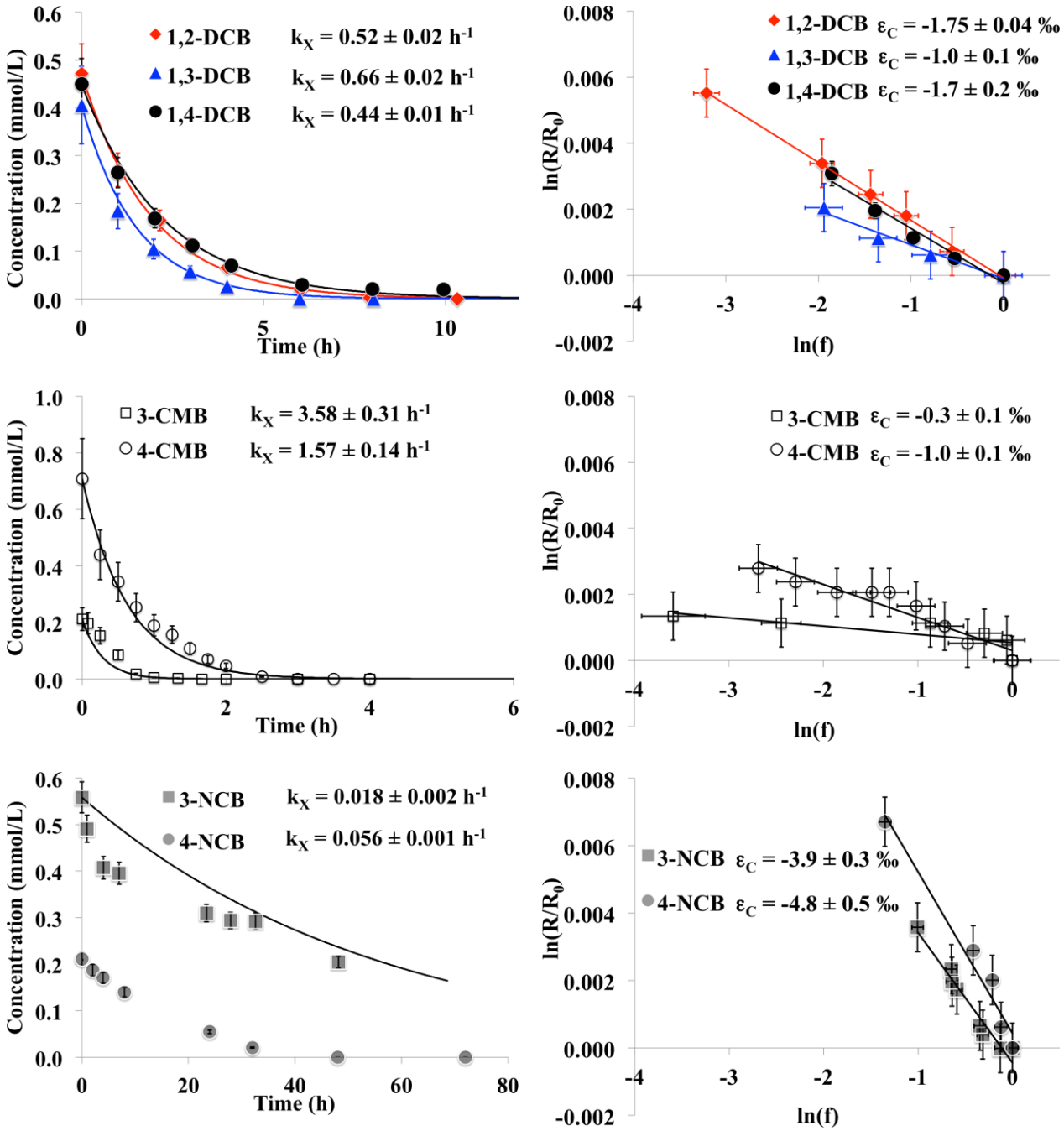

Figure 1: Concentrations (left panels) and stable carbon isotope results (linear form of the Rayleigh plot, right panels) during the reaction of the studied substituted chlorobenzenes with OH radicals. The pseudo first-order rate constants (k_X) and enrichment factors (ε_C) are presented with 95% confidence interval errors. The error bars on concentrations (2×COV, i.e. 2×coefficient of variation) were 13% (1,2-DCB), 20% (1,3-DCB), 12% (1,4-DCB), 19% (3-CMB), 20% (4-

CMB), 6% (3-NCB), and 7% (4-NCB). The error bars on stable isotope $\delta^{13}C$ values were ±0.5‰, accounting for both accuracy and reproducibility (Sherwood Lollar et al. 2007). The error bars on the Rayleigh plots were determined from error propagation. Note the differences in time intervals for the X-axis and concentration range for the Y-axis in the kinetics plots (left panels).

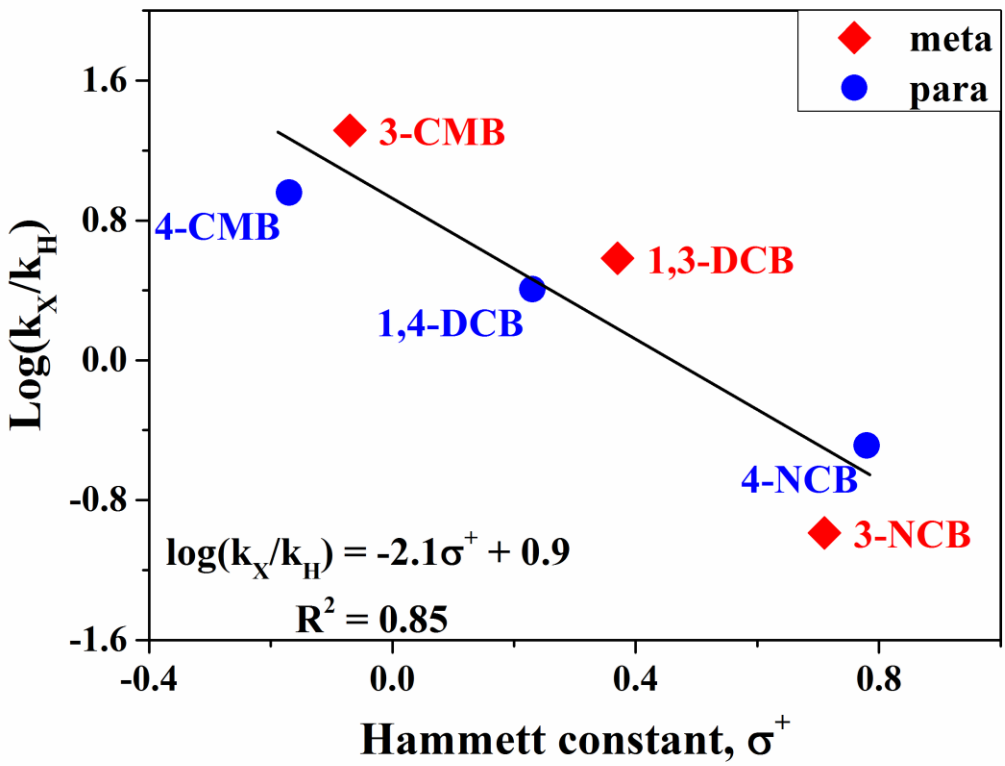

Figure 2: Hammett plot presenting the logarithm of the ratio of the pseudo first-order rate constants for the reaction between OH radicals and the non-substituted chlorobenzene (k_H, chlorobenzene), and the X-substituted chlorobenzenes (k_X, X = Cl, CH_3, and NO_2). The Hammett constant, σ^+, is the substituent constant obtained from Hansch et al (1991).

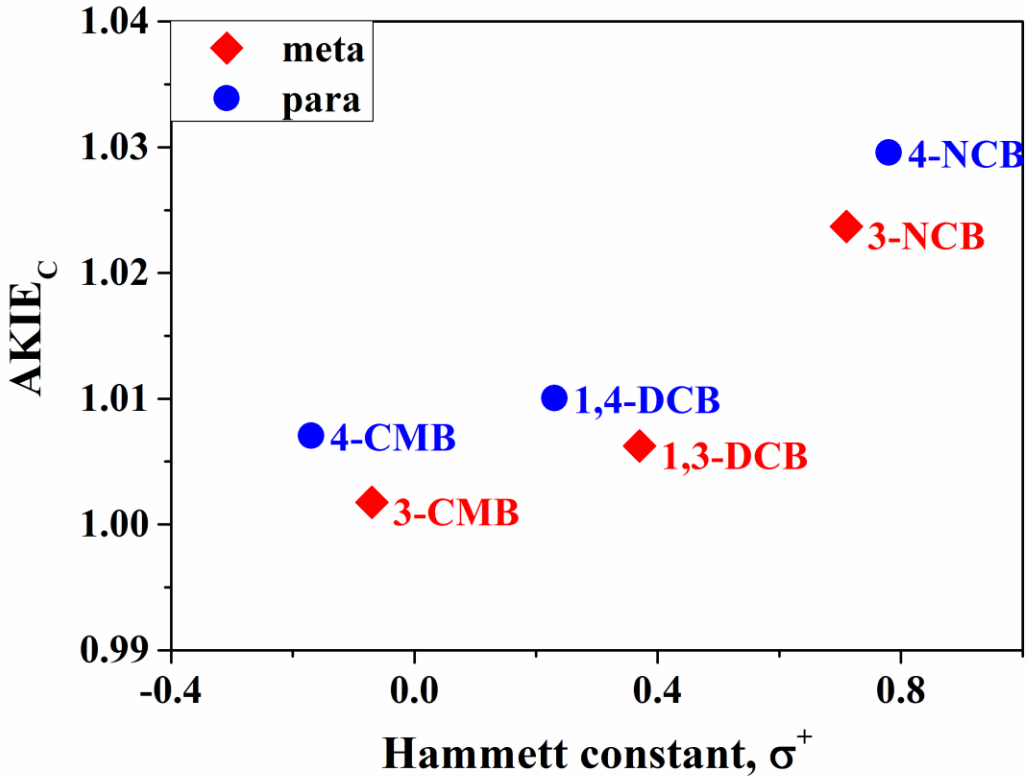

Figure 3: Correlation between $AKIE_C$ values and Hammett substituent constants for the reaction between OH radicals and the X-substituted chlorobenzenes (k_X, X = Cl, CH_3, and NO_2). The Hammett constant, σ^+, is the substituent constant obtained from Hansch et al. (1991); CMB is chloromethylbenzene, DCB is dichlorobenzene, and NCB is nitrochlorobenzene.